

## Heat capacity of hexagonal tungsten bronzes

A. J. Bevolo, H. R. Shanks, P. H. Sidles, and G. C. Danielson

Ames Laboratory and Department of Physics, Iowa State University, Ames, Iowa 50010

(Received 14 November 1973)

The heat capacity of four hexagonal tungsten bronzes ( $K_xWO_3$ ,  $Rb_xWO_3$ ,  $Cs_xWO_3$ , and  $Tl_xWO_3$ ),  $WO_3$ , and cubic  $Na_xWO_3$  have been measured from 1 to 55 K. The excess heat capacity reported by King *et al.* for  $Rb_xWO_3$  and attributed to an Einstein mode is also present in  $K_xWO_3$ ,  $Cs_xWO_3$ , and  $Tl_xWO_3$ . The values of  $x$  determined from the excess heat capacity agree reasonably well with the nominal composition having  $x = 0.33$ . The Einstein temperatures  $\Theta_E$  for the metal ions vibrating in the channels formed by the six-membered rings of  $WO_6$  octahedra were found to be 58 K for Rb, 70 K for Cs, and 38 K for Tl. Two unexplained peaks in the heat capacity of  $K_xWO_3$  near 20 K precluded an accurate determination of  $\Theta_E$  for this tungsten bronze, but  $\Theta_E$  is estimated to be between 60 and 90 K. The magnitudes of the Einstein temperatures can be understood in terms of the masses and ionic radii of the metal ions. All four hexagonal tungsten bronzes are superconductors. Measurements of the heat capacity with a magnetic field showed  $Rb_xWO_3$  to be a type-I superconductor, but  $K_xWO_3$  to be a type-II superconductor.

### I. INTRODUCTION

Tungsten bronzes are nonstoichiometric compounds with the general formula  $M_xWO_3$ , where  $M$  is a metal and  $0 < x < 1$ . The crystal structure has high symmetry for high  $x$  values and low symmetry for low  $x$  values. In all cases the structure is composed of corner-bonded  $WO_6$  octahedra with the metal ions occupying the interstitial sites. Since  $WO_3$  has a corner-bonded monoclinic structure,<sup>1</sup> the tungsten bronzes may be considered to be high-symmetry forms of  $WO_3$ , stabilized by the presence of the metal ions. If  $M$  is an alkali metal, Magneli<sup>2</sup> has shown that the hexagonal structure consists of six-member rings forming channels, and the tetragonal-I structure consists of five-member rings forming channels. The cubic structure may be considered as four-member rings.

Superconductivity was first reported by Raub *et al.*<sup>3</sup> in a tetragonal-I sodium bronze with  $x \approx 0.3$  and  $T_c$  about 0.5 K. The perovskite-related cubic and tetragonal-II structures were not superconducting. Sweedler *et al.*<sup>4</sup> reported that hexagonal K, Rb, and Cs bronzes were superconducting with  $T_c$  near 1.5 K. Remieka *et al.*<sup>5</sup> found that acid etching of the alkali-metal hexagonal bronzes increased  $T_c$  by a factor of 3, lowered the  $x$  value, and produced a contraction of the lattice along the  $c$  axis. A magnetic field of 24 kG was required to suppress  $T_c$  below 4.2 K with  $H$  parallel to the  $c$  axis. No corresponding magnetic behavior was reported for the untreated samples. Other hexagonal bronzes ( $M = Ca, Sr, Ba, In,$  and  $Tl$ ) have also been reported<sup>6,7</sup> to be superconducting with  $T_c$  from 1 to 3 K. Using a hydrothermal growth process Gier *et al.*<sup>8</sup> have been able to produce hexagonal lithium, sodium, and ammonium bronzes which are superconducting with  $T_c$  between 1 and 5.4 K.

However, they found that one hexagonal bronze,  $Sn_xWO_3$ , was not superconducting above 1 K. Superconductivity has been observed by Hubble *et al.*<sup>9</sup> in the related tungsten fluoroxide bronzes  $M_xWO_{3-x}F_x$ , where  $M = K, Rb,$  and  $Cs$  with  $x$  values from 0.08 to 0.30. They observed  $T_c$  to increase with decreasing  $x$  value, similar to the results reported for the acid-etched hexagonal bronzes. Large critical fields, 5 to 10 kG, indicative of type-II behavior were found for the Rb and Cs fluoroxide bronzes.

Low-temperature heat capacity of the tungsten bronzes has been reported by Vest *et al.*,<sup>10</sup> Gerstein *et al.*,<sup>11</sup> Kienzle *et al.*,<sup>12</sup> and King *et al.*<sup>13</sup> Vest *et al.*<sup>10</sup> have reported the specific heat of cubic  $Na_xWO_3$  for several  $x$  values from 1 to 4 K and found that  $C_p = \gamma T + \beta T^3$  with  $\gamma$  increasing with  $x$  and the Debye temperature  $\Theta_D$  (obtained from  $\beta$ ) ranging from 450 to 505 K. The Debye temperatures were obtained from  $\beta$  using  $4 + x$  as the number of atoms per formula weight. Gerstein *et al.*<sup>11</sup> measured  $C_p$  from 15 to 300 K for cubic  $Na_{0.679}WO_3$  and found a minimum in the Debye temperature at about 27 K. Kienzle *et al.*<sup>12</sup> reported on the heat capacity of five different  $Rb_xWO_3$  samples from 1 to 16 K and found  $T_c$  to be insensitive to  $x$  value within the range  $0.27 \leq x \leq 0.32$ . A low-temperature anomaly near 2 K prevented the determination of  $\gamma$  and  $\Theta_D$ . King *et al.*<sup>13</sup> have measured the heat capacity of hexagonal  $Rb_xWO_3$  with  $x \sim \frac{1}{3}$  from 1.5 to 16 K and found an excess heat capacity which they could fit to an Einstein contribution with characteristic temperature,  $\Theta_E$ , of 57 K. Since the hexagonal structure (see Fig. 1) has large channels along the  $c$  axis, which contain the  $Rb^+$  ion, it was proposed that the motion of these ions could account for the Einstein excess heat capacity. Although complicated by the presence of this excess

heat capacity and the superconducting jump in  $C_p$  near 2 K, they determined that  $\Theta_D = 415$  K and  $\gamma = 2.2$  mJ/mole K<sup>2</sup>.

We report here a systematic study of the low-temperature heat capacity of four hexagonal tungsten bronzes ( $M = \text{K, Rb, Cs, and Tl}$ ) from 1 to 55 K. Previous heat-capacity measurements on hexagonal tungsten bronzes have been reported only for  $\text{Rb}_x\text{WO}_3$ . Although critical-field measurements on acid-etched and fluorinated hexagonal bronzes suggest type-II superconductivity, no determination of the type of superconductivity has been reported for untreated tungsten bronze samples. Measurements of  $C_p$  in a magnetic field provide a clear means of distinguishing between type-I and type-II superconductivity. A magnetic field also allows one to suppress the superconducting jump in  $C_p$  so that accurate values of  $\gamma$  and  $\Theta_D$  can be obtained.

During the course of these investigations it became desirable to know  $C_p$  for  $\text{WO}_3$  from 1 to 55 K. The only available data<sup>14</sup> below room temperature were from 300 to 63 K, so we have measured  $C_p$  for  $\text{WO}_3$  from 1 to 55 K. For comparison purposes we have also measured  $C_p$  for cubic  $\text{Na}_{0.8}\text{WO}_3$  from 1 to 55 K.

## II. EXPERIMENT

Four hexagonal tungsten bronze single crystals were grown electrolytically from a fused salt.<sup>15</sup> Based on previous experience with the growth of these materials, the  $x$  values were estimated to be within 10% of 0.33, which is the upper theoretical limit for the hexagonal structure.

Mass spectrographic analyses gave similar results for all four samples. The principal impurities (relative to tungsten having 10<sup>6</sup> parts per million) were alkali metal atoms at a few thousand ppm atomic and Mo and Fe at a few hundred ppm atomic. All other impurities totaled less than 100 ppm atomic. The  $\text{WO}_3$ , grown by vapor transport, showed 2000-ppm Na and 60-ppm Mo; the sum of all other impurities was less than 20 ppm.

Heat-capacity measurements were made by the heat-pulse method in a He<sup>4</sup> cryostat of conventional design. Samples rested on a copper pan supported by nylon threads. The Ge thermometer was calibrated from 1 to 20 K on a paramagnetic-salt temperature scale,<sup>16</sup> and from 20 to 55 K on the NBS 1955 temperature scale.

A 29-g sample of 99.999% American Smelting and Refining Company (ASARCO) copper was used to determine the overall accuracy of the calorimeter. From the copper reference equation<sup>17</sup> and NBS compilation<sup>18</sup> copper from 25 to 60 K,<sup>18</sup> the measured  $C_p$  agreed within 1% of the reference  $C_p$  over the whole temperature range. The addenda correction varied from 8 to 32% for the 29-g copper

sample. For  $T < 25$  K the heat capacity of the 29 g of copper is approximately twice that of a typical bronze sample having a mass of about 8 g. Thus the estimated uncertainty in the  $C_p$  of the bronze samples is about 2%. From 25 to 55 K the heat capacity of the bronzes decreases from one-half to one-quarter that of the 29-g copper sample; so the estimated uncertainty above 25 K rises from 2% to 4%.

The magnetic field was supplied by a 12-in. Varian electromagnet. The cryostat tail was designed to fit snugly between the 2-in. gap of this electromagnet. A Hall-probe magnetometer was used to measure the applied field. Considering the homogeneity of the field and the absence of any magnetic materials near the sample, it was estimated that the field at the sample could be measured to within 1 G for fields less than 100 G.

## III. RESULTS

A normal metal at low temperatures has

$$C_p = \gamma T + \beta T^3, \quad (1)$$

where  $\gamma T$  is the electronic specific heat and  $\beta T^3$  is the lattice contribution. The lattice coefficient  $\beta$  is related to the Debye temperature  $\Theta_D$  by<sup>19</sup>

$$\beta = 1944r\Theta_D^3, \quad (2)$$

where  $\beta$  is in units of J/mole K<sup>4</sup> and  $r$  is the number of atoms per formula weight. For the bronzes  $M_x\text{WO}_3$ ,  $r = 4 + x$ . If the data are plotted as  $C_p/T$  vs  $T^2$ , Eq. (1) predicts a straight line whose slope is  $\beta$  and whose intercept is  $\gamma$ .

Heat-capacity measurements for the four hexagonal bronzes  $\text{K}_x\text{WO}_3$ ,  $\text{Rb}_x\text{WO}_3$ ,  $\text{Cs}_x\text{WO}_3$ , and  $\text{Tl}_x\text{WO}_3$  as well as for the cubic bronze  $\text{Na}_{0.8}\text{WO}_3$  and the  $\text{WO}_3$  sample are shown in Figs. 2–5. The magnetic field was less than 1 G. Our data for cubic  $\text{Na}_{0.8}\text{WO}_3$  agree with the measurements of Vest *et al.*<sup>10</sup>

In Fig. 2 the data are plotted as  $C_p/T$  vs  $T^2$  for  $1 < T < 2.8$  K. Both  $\text{Cs}_x\text{WO}_3$  and  $\text{WO}_3$  have  $\Theta_D$  equal to  $380 \pm 15$  K, while  $\text{Na}_x\text{WO}_3$  has a  $\Theta_D$  of  $520 \pm 20$  K.

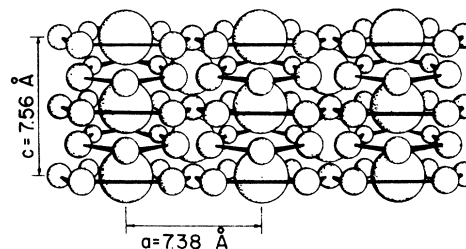


FIG. 1. Perspective view of hexagonal tungsten bronze structure (after Magneli, Ref. 2) showing open channels along the vertical  $c$  axis.

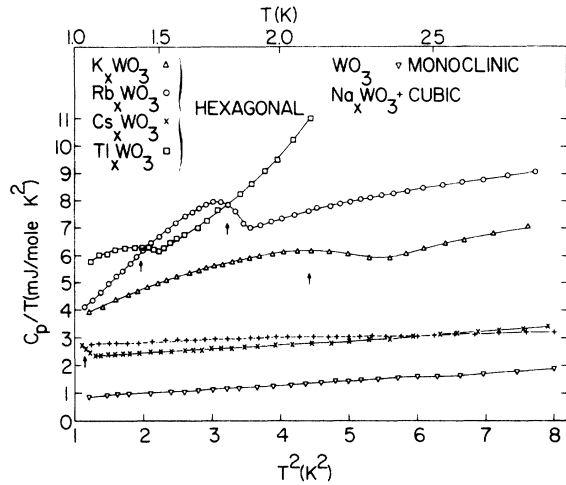


FIG. 2. Heat capacity of  $\text{WO}_3$ , cubic  $\text{Na}_x\text{WO}_3$ , and four hexagonal bronzes for  $1 < T < 2.8$  K. The superconducting transitions for the four hexagonal bronzes are shown by arrows. The plot of  $C_p/T$  vs  $T^2$  is linear for  $\text{WO}_3$ ,  $\text{Na}_x\text{WO}_3$ , and  $\text{Cs}_x\text{WO}_3$  in this temperature range.

The  $\gamma$  values, in units of  $\text{mJ/mole K}^2$ , are 0.6, 2.15, and 2.70 for  $\text{WO}_3$ ,  $\text{Cs}_x\text{WO}_3$ , and  $\text{Na}_x\text{WO}_3$ , respectively. Since  $\text{WO}_3$  is an insulator,  $\gamma$  should be zero. The origin of this linear term in the heat capacity of  $\text{WO}_3$  is unknown. Additional contributions to the heat capacity for  $\text{K}_x\text{WO}_3$ ,  $\text{Rb}_x\text{WO}_3$ , and  $\text{Tl}_x\text{WO}_3$  preclude the determination of  $\gamma$  and  $\Theta_D$  for these tungsten bronzes. In Fig. 2 the superconducting transitions for the four hexagonal bronze samples are indicated by vertical arrows.

In Fig. 3 the  $C_p$  of the same six samples are shown again in a  $C_p/T$ -vs- $T^2$  plot, but now for the temperature range  $2 < T < 6.5$  K. Only  $\text{Na}_x\text{WO}_3$  and  $\text{WO}_3$  retain their linear form. The four hexagonal bronzes show widely varying amounts of excess heat capacity with respect to the heat capacity of  $\text{Na}_x\text{WO}_3$  or  $\text{WO}_3$ . The excess heat capacity for  $\text{Rb}_x\text{WO}_3$  is qualitatively different from the excess heat capacity of the other three hexagonal bronzes below 5 K.  $\text{Rb}_x\text{WO}_3$  exhibits an added shoulderlike behavior. A magnetic field of 16 kG produced no significant change in this feature. This effect was not reported by King *et al.*,<sup>13</sup> and may be caused by impurities in our samples. Unfortunately this shoulder prevents the determination of  $\gamma$  and  $\Theta_D$  for  $\text{Rb}_x\text{WO}_3$ . The large excess  $C_p$  for  $\text{Tl}_x\text{WO}_3$  and  $\text{K}_x\text{WO}_3$  also precluded the determination of  $\gamma$  and  $\Theta_D$  for these tungsten bronzes.

Figure 4 shows the data, still plotted as  $C_p/T$  vs  $T^2$ , for temperatures up to 18 K. It is clear from these data that the  $C_p$  of the hexagonal tungsten bronzes are qualitatively different in magnitude from either  $\text{Na}_x\text{WO}_3$  or  $\text{WO}_3$ . The heat capacity of

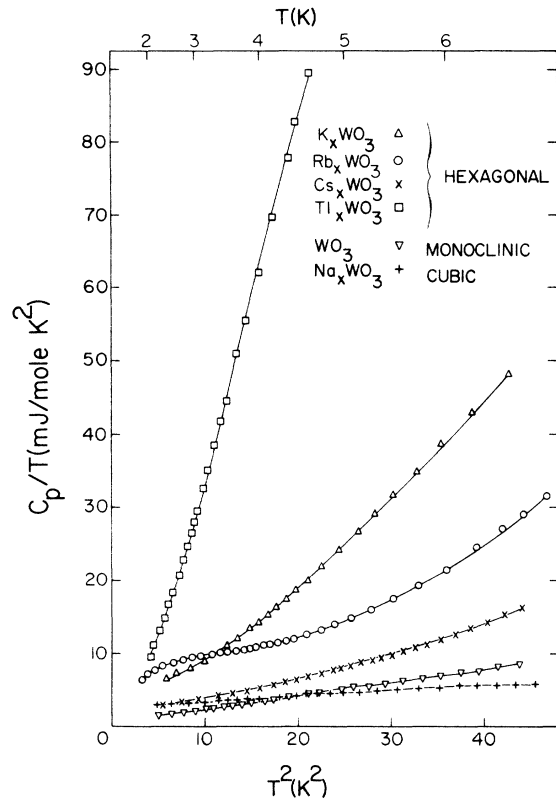


FIG. 3. Heat capacity of  $\text{WO}_3$ , cubic  $\text{Na}_x\text{WO}_3$ , and four hexagonal bronzes for  $2 < T < 6.5$  K. All four hexagonal bronzes show an excess heat capacity with respect to  $\text{WO}_3$  and  $\text{Na}_x\text{WO}_3$ , which retain their linear behavior. The excess heat capacity of  $\text{Tl}_x\text{WO}_3$  is enormous. The  $\text{Rb}_x\text{WO}_3$  curve exhibits an added shoulder.

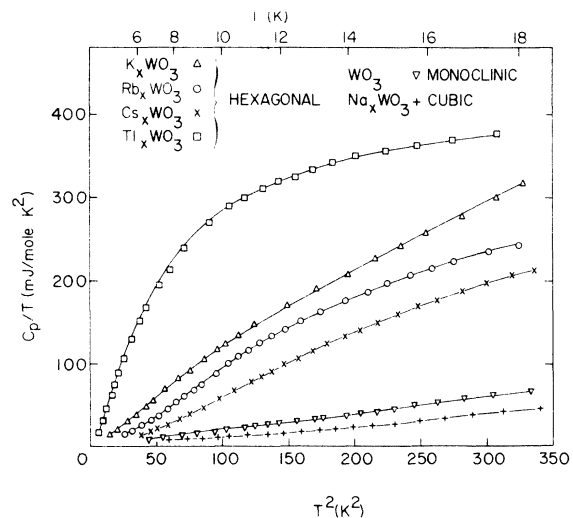


FIG. 4. Heat capacity of  $\text{WO}_3$ , cubic  $\text{Na}_x\text{WO}_3$ , and four hexagonal bronzes for  $T < 18$  K. The excess heat capacity is conspicuous for all four of the hexagonal bronzes.

$Tl_xWO_3$  is enormous compared to that of most materials.

Figure 5 shows  $C_p$  vs  $T$  up to our highest temperature, 55 K. Several new features are shown in Fig. 5. Above 40 K the difference between the heat capacity of a hexagonal bronze and the heat capacity of  $WO_3$  is nearly independent of temperature. Such is not the case for the heat capacity of  $Na_xWO_3$  which, above 40 K, appears to be converging to the heat capacity of the hexagonal bronzes. Near 20 K,  $K_xWO_3$  exhibits two closely spaced peaks in the heat capacity. These peaks occur only for this material. Measurement on three samples from the same crystal showed that neither annealing at 600 °C nor cold working nor a magnetic field of 1000 G had any influence on these peaks. A sample grown from a different fused salt exhibited a single broad peak centered at the midpoint between the two peaks shown in Fig. 5.

Figure 6 shows the heat capacity of  $Rb_xWO_3$  near the superconducting transition with the applied magnetic field perpendicular to the  $c$  axis. A prominent feature of the data in Fig. 6 is the existence of excess heat capacity near  $T_c$  in the presence of a nonzero magnetic field. These data were taken by cooling the sample to 1 K in zero magnetic field, after which the desired magnetic field was applied. At this constant magnetic field, heat capacity data were measured from 1 K to temperatures somewhat higher than  $T_c$ . Before beginning the next set of data at a different magnetic field, the field was reduced to zero and the sample warmed to at least 4.2 K. The sample was then

cooled to 1 K again in zero magnetic field, and the new field applied. This procedure was designed to eliminate any trapped flux in the sample. Data taken when the sample was cooled in a magnetic field gave evidence of trapped flux in the form of reduced excess heat capacity near  $T_c$ . The width of the transition shows a noticeable sharpening when the magnetic field is increased from zero to 7.5 G. As the field is further increased, the transition becomes broadened until at fields near 40 G the width is comparable to that observed at zero field.

The jump in heat capacity  $\Delta C$ , the transition temperature  $T_c$ , and the width of the transition  $\Delta T_c$  were obtained for each value of the magnetic field by the method shown in Fig. 7. The value of  $\Delta C$  in zero field is found to be  $4.2 \pm 0.9$  mJ/mole K. The large uncertainty in  $\Delta C$  is caused by the broadening of the transition in zero field and by the nonlinear behavior of the heat capacity in the normal state.

The critical-field curve,  $H_c$  vs  $T^2$ , for  $Rb_xWO_3$  is shown in Fig. 8. The data for zero field and for fields above 40 G are less reliable, owing to the considerable broadening of the transitions. The straight line drawn through the more reliable points (7.5 to 40 G) in Fig. 8 gives  $T_c(0) = 1.82 \pm 0.05$  K and  $H_c(0) = 94 \pm 5$  G. The error bars for the points in Fig. 9 represent the full width of the transition  $\Delta T_c$  obtained by the method shown in Fig. 7.

An unetched  $Rb_xWO_3$  sample was found to have a  $T_c$  of 2.1 K as determined by ac mutual inductance

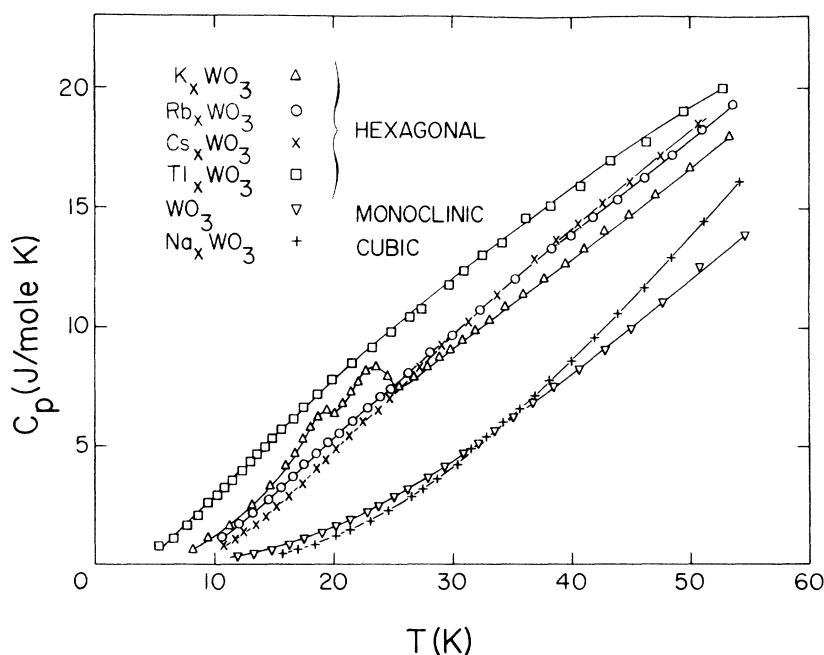


FIG. 5. Heat capacity of  $WO_3$ , cubic  $Na_xWO_3$ , and four hexagonal bronzes for  $T < 55$  K. Above 40 K the difference between the heat capacity of a hexagonal bronze and the heat capacity of  $WO_3$  is nearly independent of temperature as one would expect if this difference is due to an Einstein contribution. Near 20 K the curve for  $K_xWO_3$  exhibits two closely spaced peaks, which are unexplained.

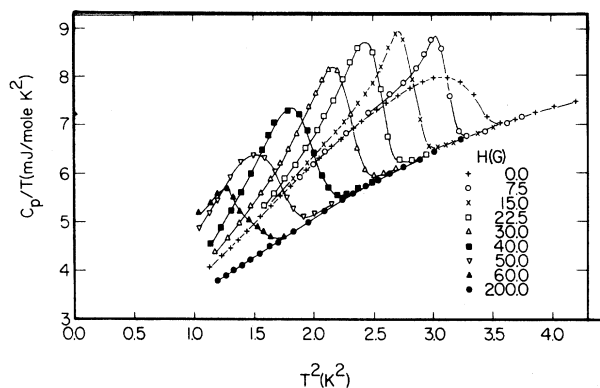


FIG. 6. Heat capacity of hexagonal  $\text{Rb}_x\text{WO}_3$  in the presence of a magnetic field. The extra heat capacity (latent heat) near  $T_c$  associated with the application of a magnetic field is characteristic of a type-I superconductor.

and by heat-capacity measurements. After treatment at  $150^\circ\text{C}$  for several hours with  $\text{H}_2\text{SO}_4$  in a pressure vessel, the mutual-inductance measurements revealed a broad superconducting transition from 3 to 5 K, while the heat capacity showed a single peak at 2.1 K. For this particular acid treatment on an  $\text{Rb}_x\text{WO}_3$  single crystal, the increase in  $T_c$  was evidently a surface effect.

#### IV. DISCUSSION

According to the model suggested by King *et al.*<sup>13</sup> the lattice heat capacity of the hexagonal bronzes consists of two parts; a lattice term due to the  $\text{WO}_6$  octahedra and an Einstein contribution due to the motion of the metal ions in the channel site. The measurement gives only the sum of these two heat-capacity contributions. In order to find the Einstein contribution, we need to obtain the  $\text{WO}_6$

lattice term by itself. An ideal solution would be to measure the heat capacity of a hexagonal-phase  $\text{WO}_3$  sample and subtract it from that of the hexagonal bronzes. The low-temperature (1–55 K) phase of  $\text{WO}_3$  is not known, but it is probably not hexagonal. However,  $\text{WO}_3$  in all its low-temperature phases has the same basic structural unit as the bronzes, namely corner-bonded  $\text{WO}_6$  octahedra.<sup>20</sup> In addition, our results for  $T < 3$  K give very similar Debye temperatures for  $\text{WO}_3$  and for the hexagonal bronze  $\text{Cs}_x\text{WO}_3$  (380 K for  $\text{WO}_3$  and 380 K for  $\text{Cs}_x\text{WO}_3$ ). Also these values of  $\Theta_D$  are very near the value of  $\Theta_D$  for  $\text{Rb}_x\text{WO}_3$  (415 K) found by King *et al.*<sup>13</sup> These results suggest that, despite the difference in crystal symmetry, the low-frequency  $\text{WO}_6$  lattice modes for  $\text{WO}_3$  and the hexagonal bronzes are very similar.

On the other hand, the low-frequency modes for cubic  $\text{Na}_x\text{WO}_3$  are not the same as for the hexagonal bronzes, and it is not appropriate to subtract the heat capacity of cubic  $\text{Na}_x\text{WO}_3$  from the heat capacity of the hexagonal bronzes to obtain the excess heat capacity. Although the fourfold  $\text{WO}_6$  bonding is nearly the same for cubic  $\text{Na}_x\text{WO}_3$  and for  $\text{WO}_3$ , the larger Debye temperature for the cubic bronze (near 500 K) suggests that the sodium ions are strongly coupled to the  $\text{WO}_6$  octahedra in  $\text{Na}_x\text{WO}_3$ . This strong coupling is not unexpected when it is noted that the metal-oxygen interatomic distance in the cubic sodium bronze (1.95 Å) is considerably smaller than that found in the hexagonal bronzes (3.29 Å).

This method of obtaining the excess heat capacity, by subtraction of  $C_p$  of  $\text{WO}_3$  from that of the hexagonal bronzes, differs from the method used by King *et al.*<sup>13</sup> in their analysis of  $\text{Rb}_x\text{WO}_3$ . They subtracted  $C_p = \gamma T + \beta T^3$  from the total heat capacity, with  $\beta$  a constant determined by measurements near 3 K. The Debye temperature, and hence  $\beta$ ,

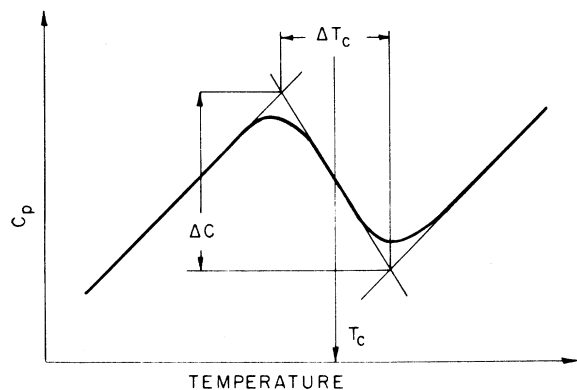


FIG. 7. Method of construction to obtain the jump in heat capacity  $\Delta C$ , the superconducting transition temperature  $T_c$ , and the width of the transition  $\Delta T_c$ .

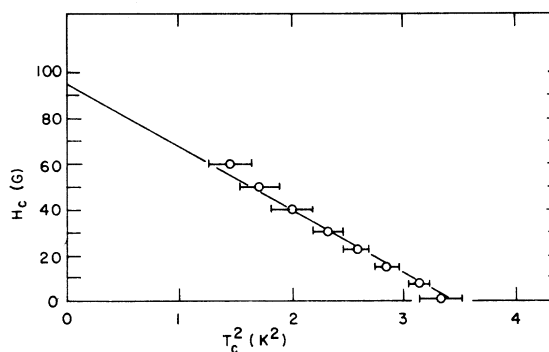


FIG. 8. Critical field curve for hexagonal  $\text{Rb}_x\text{WO}_3$ . Error bars represent the full width of the transition  $\Delta T_c$ . The straight line determines  $T_c(0) = 1.82 \pm 0.05$  K and  $H_c(0) = 94 \pm 5$  G.

is probably not a constant for the tungsten bronzes. For  $\text{WO}_3$ ,  $\Theta_D$  at 17 K is 15% smaller than  $\Theta_D$  at 3 K (or at 0 K). The assumption that  $\Theta_D$  is a constant overestimates the excess heat capacity. If  $\Theta_D$  decreases by 15%, then  $\beta$  will increase by 50%, so that the  $C_p$  subtracted may be 50% too small at the minimum in the Debye temperature.

Our method of subtracting the heat capacity of  $\text{WO}_3$  from the hexagonal bronzes will tend to compensate for the variation of  $\Theta_D$  with  $T$  and lead to a more accurate estimate of the excess heat capacity at higher temperatures.

After subtracting the heat capacity of  $\text{WO}_3$  from that of the hexagonal bronzes, we obtained the excess heat capacity shown in Fig. 9 for  $\text{Ti}_x\text{WO}_3$ ,  $\text{Rb}_x\text{WO}_3$ , and  $\text{Cs}_x\text{WO}_3$ . Although  $\text{K}_x\text{WO}_3$  has the same type of excess heat capacity (see Fig. 5), the presence of the two peaks near 20 K makes a quantitative analysis difficult. The fit of the excess-heat-capacity curves in Fig. 9 to a single Einstein heat-capacity function was tested as follows. The Einstein heat capacity can be written as

$$C_E = \frac{1}{4} C_M \alpha^2 \csc^2(\alpha/2), \quad (3)$$

where

$$C_M = 3Rs, \quad (4)$$

$R$  is the universal gas constant,  $s$  is the number of atoms per formula weight contributing to the Einstein heat capacity,

$$\alpha = \Theta_E/T, \quad (5)$$

and  $\Theta_E$  is the Einstein temperature.

Equation (3) has two unknowns,  $s$  and  $\Theta_E$ . Taking the values of excess heat capacity from the curves

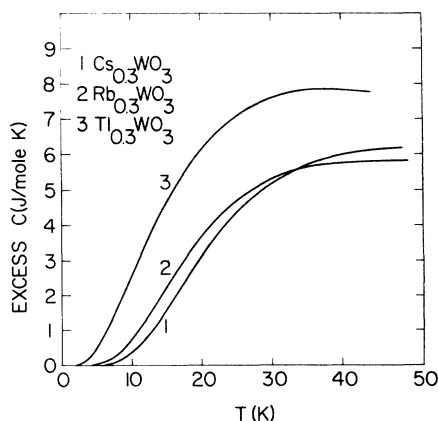


FIG. 9. Excess heat capacity of  $\text{Cs}_x\text{WO}_3$ ,  $\text{Rb}_x\text{WO}_3$ , and  $\text{Ti}_x\text{WO}_3$  obtained by subtraction of the heat capacity of  $\text{WO}_3$  from the total heat capacity. In each case, the excess heat capacity can be fitted to a single Einstein heat-capacity function.

in Fig. 9 at 10 and 30 K, two transcendental equations involving  $s$  and  $\Theta_E$  were obtained. A hyperbolic function identity allowed these two equations to be reduced to a single easily solved transcendental equation. From  $\Theta_E$  and  $s$  obtained in this manner, values of  $C_E$  at other temperatures were calculated and compared to the observed excess heat capacity. In all three cases the observed excess heat capacity could be fitted within experimental error by the values of  $\Theta_E$  and  $s$  shown in Table I.

The excess heat capacity in Fig. 9 is given to temperatures only up to 45 K, because the excess heat capacity becomes a smaller part of the total heat capacity with increasing temperature. In addition, the germanium thermometer has less sensitivity at the higher temperatures. These two effects combine to increase the error in the excess heat capacity from 4% at the lower temperatures to 8% at 45 K.

The agreement between the  $x$  values of these three samples and the  $s$  values obtained from the excess heat capacity confirms the hypothesis that this excess heat capacity is due to the metal ions.

For these temperatures ( $T < 55$  K) the metal ions can be thought of as a collection of nearly independent particles executing three-dimensional simple harmonic motion with frequency

$$\nu_E = k_B \Theta_E / h, \quad (6)$$

where  $k_B$  is the Boltzmann constant and  $h$  is Planck's constant. The frequency of vibration is

$$\nu_E = (\frac{1}{2} \pi) (k/m)^{1/2}, \quad (7)$$

where  $k$  is the force constant associated with the restoring forces acting on the  $M^+$  ions and  $m$  is the mass of the  $M^+$  ions. Solving Eqs. (6) and (7) for  $\Theta_E$ , we obtain

$$\Theta_E = (\hbar/k_B) (k/m)^{1/2}. \quad (8)$$

The masses of the metal ions are well known and are given in Table I in amu. The force constants calculated from these masses and the measured values of  $\Theta_E$  are shown in Table I.

The volume of a channel site containing the metal ion does not change appreciably from one hexagonal bronze to another, since the unit-cell dimensions (see Table I) do not change. Thus the overlap of the  $M^+$  ion orbitals with the nearest-neighbor-oxygen orbitals, which presumably produces the restoring force, will depend primarily on the ionic radius of the  $M^+$  ion. The larger the  $M^+$  ion, the greater the overlap and the greater the force constant  $k$ . This conclusion, that  $k$  depends largely on the ionic radius, helps to account for some of the numbers in Table I. Both the  $\text{Ti}^+$  and  $\text{Rb}^+$  ions have the same ionic radius, and they do indeed have the same force constant. Also consider  $\Theta_E$  of  $\text{Rb}_x\text{WO}_3$  and  $\text{Cs}_x\text{WO}_3$ . The heavier  $\text{Cs}^+$  ion

should, by Eq. (8), produce a smaller  $\Theta_E$  for the same  $k$ . The fact that  $\Theta_E$  for  $\text{Cs}_x\text{WO}_3$  is larger than  $\Theta_E$  for  $\text{Rb}_x\text{WO}_3$  can be explained by its larger ionic radius, which produces a larger force constant. These simple assumptions give a qualitative understanding of  $\Theta_E$  for the hexagonal tungsten bronzes.

It is difficult to determine  $\Theta_E$  for  $\text{K}_x\text{WO}_3$  in the presence of the large peaks near 20 K. However, we can make a fair estimate of  $\Theta_E$  for  $\text{K}_x\text{WO}_3$ . The ionic radius of  $\text{K}^+$  is 1.33 Å, which is smaller than  $\text{Rb}^+$ , so we expect a smaller force constant for  $\text{K}_x\text{WO}_3$ . A maximum value of 90 K for  $\Theta_E$  of  $\text{K}_x\text{WO}_3$  is obtained from Eq. (8) with  $m = 39.1$  amu and  $k$  equal to the value for  $\text{Rb}_x\text{WO}_3$ . To obtain a minimum value of  $\Theta_E$  for  $\text{K}_x\text{WO}_3$ , we observe from Fig. 6 that for  $T > 30$  K the heat capacity of  $\text{K}_x\text{WO}_3$  is less than the heat capacity of  $\text{Rb}_x\text{WO}_3$ . This lower value for  $\text{K}_x\text{WO}_3$  is probably caused primarily by a high  $\Theta_E$  rather than by a low  $x$  value, since the nominal  $x$  value for  $\text{K}_x\text{WO}_3$  is 0.33, which is higher than the  $x$  value for  $\text{Rb}_x\text{WO}_3$ . Thus  $\Theta_E$  for  $\text{K}_x\text{WO}_3$  is larger than  $\Theta_E$  for  $\text{Rb}_x\text{WO}_3$  (57 K). The Einstein temperature for hexagonal potassium tungsten bronze very likely lies between 60 and 90 K.

The anomalous peaks in the heat capacity of  $\text{K}_x\text{WO}_3$  are not understood. They may be due to impurities, although their existence in four samples (two different melts) makes this explanation doubtful. The peaks might be caused by latent heat from a low-temperature change in crystal structure. X-ray diffraction near 20 K would be desirable to investigate this possibility.

Considering the structure of the channel site which contains the  $M^+$  ion, one would expect an anisotropy in the force constants which would lead to two Einstein temperatures. McColm *et al.*<sup>21</sup> have obtained the Mössbauer spectra at low temperature ( $T \sim 4.2$  K) for hexagonal  $\text{Sn}_x\text{WO}_3$ . These spectra show anisotropy which the authors attribute

TABLE I. Einstein temperatures  $\Theta_E$  and related data for three hexagonal bronzes.  $\Theta_E$  and  $s$ , the number of atoms per formula weight contributing to the excess heat capacity, are obtained from curves shown in Fig. 9. The mass and ionic radius of the metal ions are given by  $m$  and  $R$ , respectively. The force constants  $k$  are obtained from  $m$  and  $\Theta_E$  using Eq. (8). The dimensions of the unit cell are  $c$  and  $a$ .

	$\text{Rb}_x\text{WO}_3$	$\text{Cs}_x\text{WO}_3$	$\text{Tl}_x\text{WO}_3$
$\Theta_E$ (K)	$58 \pm 2$	$70 \pm 3$	$38 \pm 3$
$s$	$0.29 \pm 0.02$	$0.32 \pm 0.02$	$0.33 \pm 0.02$
$m$ (amu)	86	133	204
$k$ (N/m)	8	19	8
$c$ (Å)	7.56	7.60	7.52
$a$ (Å)	7.38	7.41	7.38
$R$ (Å)	1.49	1.65	1.49

to anisotropy of the metal-ion motion in the channel sites. Within the errors in  $\Theta_E$  shown in Table I we find no such anisotropy in the K, Rb, Cs, and Tl hexagonal bronzes.

Our value for the Debye temperature of hexagonal  $\text{Cs}_x\text{WO}_3$  (380 K) is about the same value (415 K) King *et al.*<sup>13</sup> obtained for hexagonal  $\text{Rb}_x\text{WO}_3$ . In contrast the value of  $\Theta_D$  for cubic  $\text{Na}_x\text{WO}_3$  is about 500 K. This lower value of  $\Theta_D$  for the hexagonal structure is expected, owing to the reduced coupling of the metal ions to the  $\text{WO}_6$  octahedra in the hexagonal structure.

Comparison of the heat capacity of  $\text{Rb}_x\text{WO}_3$  in a magnetic field near  $T_c$  (see Fig. 6) with the classical calculations of Peierls<sup>22</sup> clearly reveals the latent heat associated with type-I superconductivity. We conclude that  $\text{Rb}_x\text{WO}_3$  is a type-I superconductor. Although  $\gamma$  could not be determined directly for  $\text{Rb}_x\text{WO}_3$ , owing to the anomalous hump in the heat capacity, a not-unrealistic  $\gamma$  of 1.9 mJ/mole  $\text{K}^2$  gives a jump in heat capacity  $\Delta C = 1.43\gamma T_c$  in accord with BCS<sup>23</sup> theory at  $H = 0$ . From the critical-field curve of  $\text{Rb}_x\text{WO}_3$ , we obtain  $(dH_c/dT)_{T=T_c} = 94 \pm 5$  G/K, and  $T_c = 1.82$  K at  $H = 0$ . The molar volume  $V$  of  $\text{Rb}_x\text{WO}_3$  is 26 (cm)<sup>3</sup>/mole. From Rutgers's formula<sup>24</sup>

$$\Delta C = \left( \frac{VT_c}{4\pi} \right) \left( \frac{dH}{dT} \right)_{T=T_c}^2, \quad (9)$$

we calculate a jump in specific heat of 4.6 mJ/mole K in agreement with the experimental value  $4.2 \pm 0.9$  mJ/mole K.

Data (not shown) for  $C_p$  of  $\text{K}_x\text{WO}_3$  in a magnetic field are marred by large irreversible heating effects. However, no latent heat was found at  $T = T_c$ , which implies type-II superconductivity. While a field of approximately 300 G was required to suppress  $T_c$  below 1 K for  $\text{K}_x\text{WO}_3$ , a field of only 100 G was required for  $\text{Rb}_x\text{WO}_3$ . Because of the possible effects of impurities it is not known whether pure  $\text{K}_x\text{WO}_3$  is an intrinsic type-I or type-II superconductor.

At low temperatures ( $T \sim \Theta_E$ ) the Einstein modes dominate the phonon spectra of the hexagonal tungsten bronzes. Properties such as superconductivity, thermal conductivity, Debye-Waller factor,<sup>25</sup> and inelastic neutron scattering may be strongly affected by these Einstein modes. A crude estimate may be made of the relative numbers of Einstein modes of the metal ions to the Debye modes of the  $\text{WO}_6$  octahedra excited at the Einstein temperature. The number of Einstein modes  $N_E = 3N_0 x$ , where  $N_0$  is Avogadro's number. The number of Debye modes, if we assume the density of states  $g(\nu) = 9N_0\nu^2/\nu_D^3$ , is

$$N_D = \int_0^{\nu_E} g(\nu) d\nu = 3N_0(\Theta_E/\Theta_D)^3. \quad (10)$$

The ratio  $N_E/N_D = x(\Theta_E/\Theta_D)^3$ . For  $x=0.3$  and  $\Theta_D = 400$  K,  $N_E/N_D$  is 100 for  $\text{Rb}_x\text{WO}_3$ , 60 for  $\text{Cs}_x\text{WO}_3$ , and 400 for  $\text{Tl}_x\text{WO}_3$ . The Einstein modes are much more numerous than the Debye modes near the Einstein temperature.

It is tempting to suggest that the large number of Einstein phonon modes generated by the  $M^+$  ions in the hexagonal bronzes may be responsible for their superconductivity through an enhanced electron-phonon interaction. The tetragonal-I bronzes, with  $T_c$  near 0.5 K, have five-, four-, and three-member channel sites in their structure. One would expect that the smaller five-member rings, when occupied by the  $M^+$  ions, would produce larger force constants than those associated with the six-member sites of the hexagonal structure. These larger force constants would lead to higher  $\Theta_E$ , which would reduce the number of phonon modes at low temperatures and thereby lower  $T_c$ , as observed. The perovskite structure, characteristic of the cubic bronzes which are not superconducting, has still smaller four-member channel sites. Indeed the metal ions become strongly coupled to the  $\text{WO}_6$  octahedra. The higher force constants would lead to an even higher  $\Theta_E$ . Therefore, we would expect a  $T_c$  lower than the  $T_c$  associated with the tetragonal-I structure. Thus a mechanism based on an enhanced electron-phonon interaction arising from the vibration of the  $M^+$  ions in the various-size channel sites seems to account for the structure dependence of the superconductivity of the tungsten bronzes.

However, closer inspection of this model leads to difficulties. A clear prediction of this mechanism is that  $T_c$  ought to scale inversely with  $\Theta_E$ . In fact,  $\text{Tl}_x\text{WO}_3$  has  $T_c$  lower than  $T_c$  for  $\text{K}_x\text{WO}_3$  or  $\text{Rb}_x\text{WO}_3$ , and its  $\Theta_E$  is also lower. The increase

in  $T_c$  with decreasing  $x$  value observed for acid-etched samples is also exactly opposite to what should occur. The fewer the  $M^+$  ions the fewer the phonon modes and  $T_c$  should decrease. On the whole the Einstein phonon modes associated with the  $M^+$  ions can be considered, at best, as only partly effective in accounting for the superconducting properties of the tungsten bronzes.

## V. CONCLUSIONS

An excess heat capacity has been observed in four hexagonal tungsten bronzes. Choosing  $\text{WO}_3$  as a reference, quantitative analysis of this excess heat capacity for three samples ( $\text{Rb}_x\text{WO}_3$ ,  $\text{Cs}_x\text{WO}_3$ , and  $\text{Tl}_x\text{WO}_3$ ) in the temperature range 1 to 45 K gave an Einstein contribution characterized by a single Einstein temperature. This excess heat capacity has been shown to result from the vibration of the  $M^+$  ions in the hexagonal channel sites. A semiquantitative understanding of the size of the Einstein temperatures has been obtained from an analysis involving the mass and ionic radius of the  $M^+$  ion. The phonon spectra of the hexagonal bronzes at low temperatures are dominated by these local Einstein phonon modes and should have dramatic effects on some of the other low-temperature properties of these materials.

## ACKNOWLEDGMENTS

We are indebted to D. K. Finnemore for many helpful discussions. We wish to thank W. E. Kienzle for design and construction of the heat-capacity apparatus, J. A. Tunheim for assistance with some of the experiments, and D. E. Eckels for designing the computer programs. We wish to express our appreciation to C. N. King for a report prior to publication.

<sup>1</sup>G. Andersson, *Acta. Chem. Scand.* **7**, 154 (1953).

<sup>2</sup>A. Magneli, *Nature* **169**, 791 (1952).

<sup>3</sup>Ch. J. Raub, A. R. Sweedler, M. A. Jensen, S. Broadston, and B. T. Matthias, *Phys. Rev. Lett.* **13**, 746 (1964).

<sup>4</sup>A. R. Sweedler, Ch. J. Raub, and B. T. Matthias, *Phys. Lett.* **15**, 108 (1965).

<sup>5</sup>J. P. Remeika, T. H. Geballe, B. T. Matthias, A. S. Cooper, G. W. Hull, and E. M. Kelley, *Phys. Lett.* **24A**, 565 (1967).

<sup>6</sup>P. E. Bierstedt, T. A. Bither, and F. J. Darnell, *Solid State Commun.* **4**, 25 (1966).

<sup>7</sup>A. R. Sweedler, J. K. Hulm, B. T. Matthias, and T. H. Geballe, *Phys. Lett.* **19**, 82 (1965).

<sup>8</sup>T. E. Gier, D. C. Pease, A. W. Sleight, and T. A. Bither, *Inorg. Chem.* **8**, 1646 (1968).

<sup>9</sup>F. F. Hubble, J. M. Gulick, and W. G. Moulton, *J. Phys. Chem. Solids* **32**, 2345 (1971).

<sup>10</sup>R. W. Vest, M. Griffel, and J. F. Smith, *J. Chem. Phys.* **28**, 293 (1958).

<sup>11</sup>B. C. Gerstein, A. H. Klein, and H. R. Shanks, *J. Phys. Chem. Solids* **25**, 177 (1964).

<sup>12</sup>W. E. Kienzle, A. J. Bevolo, G. C. Danielson, P. W. Li, H. R. Shanks, and P. H. Sidles, in *Proceedings of the Thirteenth International Conference on Low Temperature Physics, Boulder, Colo.* 1972, edited by R. H. Kropschot and K. D. Timmerhaus (University of Colorado Press, Boulder, Colo., 1973).

<sup>13</sup>C. N. King, T. A. Benda, W. A. Phillips, and T. H. Geballe, in Ref. 12.

<sup>14</sup>H. Seltz, F. J. Dunkerley, and B. J. DeWitt, *J. Amer. Chem. Soc.* **65**, 600 (1943).

<sup>15</sup>H. R. Shanks, *J. Cryst. Growth* **13/14**, 433 (1972).

<sup>16</sup>C. A. Swenson, *Metrologia* **9**, 99 (1973).

<sup>17</sup>D. W. Osborne, H. E. Flotow, and F. Schreiner, *Rev. Sci. Instrum.* **38**, 159 (1967).

<sup>18</sup>G. T. Furukawa, W. G. Saba, and Martin L. Reilly, *Natl. Stand. Ref. Data Ser.* **18**, 1 (1968).

<sup>19</sup>E. S. R. Gopal, *Specific Heats at Low Temperature* (Plenum, New York, 1966), p. 31.



<sup>20</sup>S. Tanisaki, J. Phys. Soc. Jap. 15, 566 (1960).

<sup>21</sup>I. J. McColm, R. Steadman, and A. Howe, J. Solid State Chem. 2, 555 (1970).

<sup>22</sup>R. Peierls, Proc. Roy. Soc. A 155, 613 (1936).

<sup>23</sup>J. Bardeen, L. N. Cooper, and J. R. Schrieffer, Phys.

Rev. 108, 1175 (1957).

<sup>24</sup>D. Schoenberg, *Superconductivity* (Cambridge U. P., Cambridge, England, 1962), p. 60.

<sup>25</sup>J. Goodenough (private communication).